JOURNAL OF Applied Polymer SCIENCE

Layer-by-Layer Assembled Hydrogel Nanocomposite Film with a High Loading Capacity

Renbao Gu, Xinglin Yuan, Ronglan Wu, Huili Li, Shimei Xu, Jide Wang
Key Laboratory of Oil and Gas Fine Chemicals, Ministry of Education, Xinjiang University, Urumqi, Xinjiang, 830046, People's Republic of China
Correspondence to: S. Xu (E-mail: xushmei@gmail.com)

ABSTRACT: The layer-by-layer assembly technique is a method that widely used in the preparation of nanostructured multilayer ultrathin films. We fabricated a hydrogel nanocomposite film by alternating the deposition of a core–shell poly[(dimethylimino) (2-hydroxy-1,3-propanedily) chloride] (PDMIHPC)–laponite solution and poly(acrylic acid). The growth of the deposition procedure was proven by ultraviolet–visible spectroscopy and spectroscopic ellipsometry. The surface morphology of the films was observed by scanning electron microscopy. The films could reversibly load and release methylene blue (MB) dye, which was used as an indicator. It took about 4.5 h to reach loading equilibrium at pH 9.0. The loading capacity of the film for MB was as large as 4.48 μg/cm^2 per bilayer because of the introduction of the core–shell PDMIHPC–laponite as a film component. Nearly 90% of MB was released at pH 3.0 or in a 300 m*M* NaCl solution within 2.5 h. The loading and release processes were greatly influenced by the ionic strength and pH value of the MB solution. The hydrogel nanocomposite film showed good pH-triggered loading-release reversibility and suggested potential applications in controlled drug-delivery systems and smart materials. © 2013 Wiley Periodicals, Inc. J. Appl. Polym. Sci. **2014**, *131*, 39352.

KEYWORDS: adsorption; drug-delivery systems; films; gels; self-assembly

Received 4 December 2012; accepted 20 March 2013
DOI: 10.1002/app.39352

INTRODUCTION

In recent years, a lot of work has been done to improve sustained and controlled drug-delivery systems.[1,2] It is vitally important to construct polymeric matrices with a high loading of bioactive molecules and controllable release under physiological conditions. The layer-by-layer (LbL) assembly technique is one of the easiest ways to fabricate nanostructured multilayer ultrathin films with precise control of the film thickness and composition.[3–5] The general concept of multilayer formation is electrostatic attraction,[6] and it has been expanded to alternating films stabilized by hydrogen bonding,[7–9] covalent bonding,[10] hydrophobic interactions,[11] and molecular recognition.[10] A large number of components can be used to fabricate multilayer assemblies, including water-soluble polyelectrolytes,[12–14] natural polymers (e.g., DNA, RNA, proteins, peptides, enzymes, and polysaccharides),[15–18] and advanced materials (e.g., synthetic polymers, dendritic molecules, and nanoparticles).[19–25]

Much attention has been paid to the loading and release of guest materials within LbL-assembled multilayer films.[2,26,27] It is a challenge to increase the loading capacity of the LbL films. A microcapsule technique developed by Caruso and coworkers[28,29] could be used in LbL films and showed the reversible loading and release of guest materials in many applications. In addition, LbL films containing microgel components or branched polymers have been considered particularly noteworthy.[30–32] Sun et al.[13] and coworkers synthesized a new type of microgel [poly(allylamine hydrochloride)–dextran (PAH–D)] by crosslinking poly(allylamine hydrochloride) (PAH) and dextran. Then, the polyampholyte microgel [poly(allylamine hydrochloride)–dextran (PAH–D)–CO_2 (PAH–D–CO_2)] was obtained by the bubbling of CO_2 into the PAH–D solution and was LbL-assembled with poly(sodium 4-styrenesulfonate) (PSS) to produce PAH–D–CO_2/PSS multilayer films. The loading of methyl orange in the film reached its maximum of about 0.23 μg/cm^2 per bilayer. Chung and Rubner[2] showed that the methylene blue (MB) loading capacity of PAH/poly(acrylic acid) (PAA) films was about 0.79 μg/cm^2 per bilayer. In contrast, Sun et al.[33] fabricated an LbL PAH–D/PSS film, which had a loading capacity for methyl orange as large as 3.0 μg/cm^2 per bilayer. The films could be swollen or shrunken in response to various external stimuli, such as temperature, pH, and ionic strength of the solution, and showed the specific characteristic of bulk hydrogels. Moreover, because of their small size, the hydrogel films were

expected to be highly sensitive and provide a wide prospection in actual application compared with traditional hydrogels.

In our previous study, a multilayer film assembled from polyurethane and PAA showed the controlled loading and release of MB.[34] In this study, we tried to change a linear film component to a three-dimensional component in an attempt to increase the loading capacity. Our work was also motivated by a mechanically strong nanocomposite hydrogel, which was prepared by the crosslinking polymerization of acrylic acid (AA) in the dispersion of a core–shell poly[(dimethylimino)(2-hydroxy-1,3-propanedily) chloride] (PDMIHPC)–laponite nanocomposite.[35] So, PDMIHPC–laponite with a core–shell structure was chosen as one of two film components in attempt to increase the interlayer spacing, whereas PAA was selected as the other film component for the fabrication of a loose structure. As a result, the final hydrogel nanocomposite film was expected to facilitate the incorporation of the guest materials and guaranteed an increased amount of guest materials loaded. In this study, the hydrogel nanocomposite film was investigated with regard to the loading and release of MB, which was selected as an indicator. We found that the film had a high loading capacity. Both the loading and releasing processes were controlled by the ionic strength and pH value of the immersing solution. The film showed good reversibility with pH changes.

EXPERIMENTAL

Materials and Sample Preparation

Dimethylamine (33% aqueous solution) was purchased from Shanghai Chemical Co., Ltd. Epichlorohydrin was obtained from Tianjin Fuchen Chemistry Reagent Factory. Laponite XLG [$Mg_{5.34}Li_{0.66}Si_8O_{20}(OH)_4Na_{0.66}$] was obtained from Rock Wood Co., Ltd. The PDMIHPC–laponite solution was prepared according to our previous work.[35] PAA (weight-average molecular weight = 240,000, 25 wt %) was purchased from Alfa Aesar China Co., Ltd. (Tianjin, China). MB was obtained from Tianxin Chemical Co. (Tianjin, China). Sodium chloride was purchased from Beijing Chemical Reagent Co. (Beijing, China). The pH value of the MB solution was adjusted with either HCl or NaOH solution. Deionized (DI) water was used in all of the experiments, and all other chemicals and solvents were analytical grade and were used without any further purification.

Glass slides and silicon substrates were sonicated with a Kunshan KQ5200 sonicator. Then, the samples were cleaned with fresh piranha solution (a 3:1 v/v mixture of 98% H_2SO_4 and 30% H_2O_2) for 40 min (piranha solution is extremely dangerous and had to be handled very carefully), then thoroughly washed with DI water, and finally dried under air flow.

Multilayer Film Assembly

We prepared the multilayer films by alternating the deposition of PDMIHPC–laponite and PAA onto the glass substrates. The concentration of polycation was 48 mg/mL, and that of the polyanion was 10 mg/mL. The substrates were first immersed in PDMIHPC–laponite for 3 min; this was followed by rinsing in two separate baths of DI water for 1 min, respectively, and drying under air flow. The substrates were then immersed in PAA for 3 min, and this was followed by the same rinse cycle. This entire process was repeated with the final deposited layer of PAA unless otherwise noted. The films were assembled from a total of 10 bilayers, which is denoted as (PDMIHPC–laponite/PAA)$_{10}$.

Characterization

The measurements of the film thickness were performed with a SC620 spectroscopic ellipsometer (Shanghai, China). All of the measurements were done at three angles of incidence: 45, 60, and 75°. Optical characterization was carried out with a UV 2550 spectrophotometer (Shimadzu, Japan). Fourier transform infrared (FTIR) spectra were recorded on a Bruker Equinox55. The surface and cross section of the film were observed with a LEO 1450VP scanning electron microscope. The cross section was obtained by cutting from the film side with a cutter.

Loading and Release of MB

The glass slides coated with LbL films were immersed into 0.1 mg/mL MB solutions at different pH values. The films were taken out after a given time, then rinsed with DI water to remove excess MB molecules, and dried under an airflow. The loading process of MB in the (PDMIHPC–laponite/PAA)$_{10}$ film was monitored by ultraviolet–visible (UV–vis) absorption spectroscopy.

The release of MB was carried out with a (PDMIHPC–laponite/PAA)$_{10}$ film loaded with MB, which was prepared by immersion of the film in a 0.1 mg/mL MB solution (pH 9.0) for 5 h and then drying. The (PDMIHPC–laponite/PAA)$_{10}$ film loaded with MB was immersed into aqueous solutions with various NaCl concentrations and various pH values. The solutions were mechanically stirred during the release process. The amounts of MB released from the films were determined by UV–vis spectroscopy at regular intervals. The immersing solutions were frequently replaced by fresh ones to ensure accurate absorbance readings. All measurements were carried out at room temperature (ca. 20°C).

RESULTS AND DISCUSSION

Film Assembly

The LbL films were assembled on glass slides, and the piranha treatment allowed the removal of residues of organic impurities from the substrates and made the slides completely hydrophilic at the same time.[36] The driving force for the LbL film was the electrostatic interaction and physical embedment between PDMIHPC–laponite and PAA. During the deposition process of the (PDMIHPC–laponite/PAA)$_{10}$ film, the transparency decreased with increasing deposition cycles in general, but the deposition of the PDMIHPC–laponite solution was accompanied by an increase in the transparency compared with subsequent deposition of PAA. UV–vis absorption spectroscopy was used to verify the phenomenon (Figure 1). It indicated the absorbance dependence of the growth of the layers of PDMIHPC–laponite [Figure 1(a)] and the layers of PAA [Figure 1(b)], respectively. The inset in Figure 1(b) shows the absorbance of each layer at 400 nm. The alternating assembly of PDMIHPC–laponite and PAA increased the thickness of the film and decreased the transparency. However, the core–shell nanostructure of PDMIHPC–laponite led to potential spaces within the

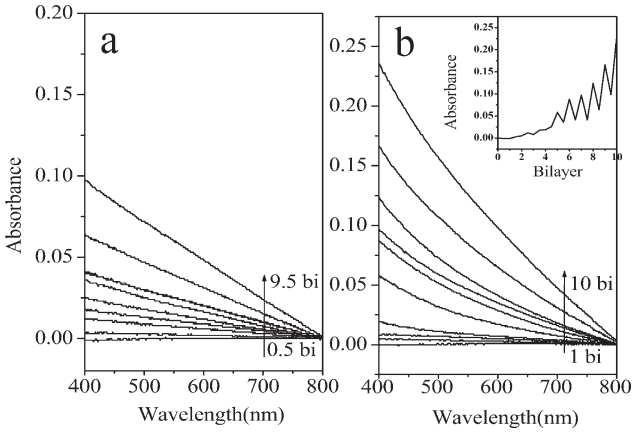

Figure 1. UV–vis absorption spectra of the LbL assembly process. The absorbance of the layers of (a) PDMIHPC–laponite and (b) absorbance of the layers of PAA. The inset shows the absorbance of each layer at 400 nm.

layer and interlayers, so the subsequent deposition of PDMIHPC–laponite compacted the previous space and hence reduced the absorbance accordingly.

A vast majority of polyelectrolyte films undergo linear growth. Exponential growth of a film was observed by Elbert et al.[37] for the first time in 1999.[6] To estimate the growth of the hydrogel nanocomposite film, an ellipsometer was used to monitor the layer thickness after the layer deposition step. As shown in Figure 2, the LbL films displayed a linear buildup from 4 to 10 bilayers after the initial few bilayers were deposited onto the substrates; this could be described as $d = 109.3n - 359.7$ ($R^2 = 0.9967$), where d is the thickness and n is the number of bilayers. The surface effect of the substrates resulted in the first nonlinear growth observed for the first few bilayers. It influenced the amount of polymer adsorbed and the conformation of the polymer on the substrates. The layer of the films became thicker after the nonlinear growth process; this implied that the layers of polyelectrolytes were absorbed on the surface in a consistent and constant manner. We deduced that the architecture of the polyelectrolytes through the bulk of the film should have been uniform, and the density of the film was homogeneous.

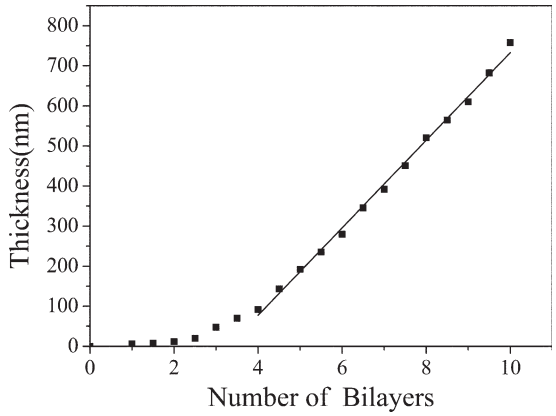

Figure 2. Growth curve of the PDMIHPC–laponite/PAA hydrogel nanocomposite film.

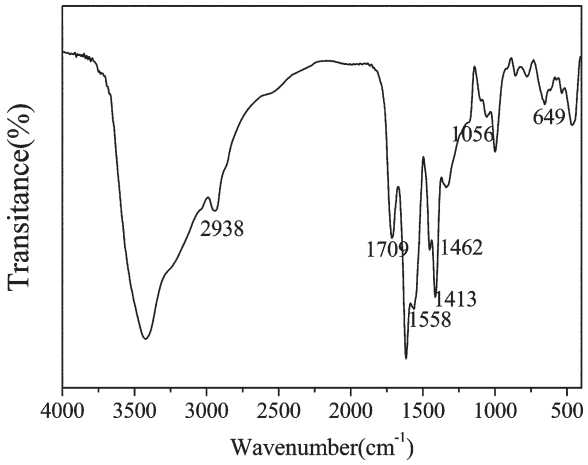

Figure 3. FTIR spectra of the (PDMIHPC–laponite/PAA)$_{10}$ hydrogel nanocomposite films.

Tsukruk et al.[38] fabricated poly[2-(dimethylamino) ethylmethacrylate] and PAA multilayer films at pH 6 and observed that the linear range of the film was from 9 to 30 bilayers. In our experiment, the rate of growth in the film was around 100 nm per bilayer.

The FTIR spectrum of the polyelectrolyte film was taken to verify the assembly of PDMIHPC–laponite and PAA (Figure 3). The bands appearing at 1056 and 649 cm^{-1} were ascribed to Si—O stretching and Si—O bending modes. An peak at 1709 cm^{-1} was assigned to the stretching vibrations of the —COOH of PAA segment. The bands founded at 1413 and 1558 cm^{-1} were due to the peaks of —COO^- asymmetric and symmetric stretching. So, we concluded that the film was composed of PDMIHPC–laponite and PAA.

Loading of MB

The maximum absorbance (λ_{max}) of MB in aqueous solution was 664 nm, with a shoulder at 615 nm. The films had no absorption peaks in the range 400–800 nm. After the film loading with MB, λ_{max} of MB in the film blueshifted to 595 nm because of the aggregation of MB.[39] A similar blueshift was observed by Chung and Rubner[2] and Ding et al.[34] The phenomenon in which the aggregation of dyes led to a blueshift in λ_{max} can be found in many dyes. This is due to stronger interaction and directional alignment between aggregated dyes. When the MB loading time increased, the intensity of the absorbance increased. As a result, the absorbency of MB could be used to estimate the amount of MB in the film.

The presence of the weakly acidic and basic groups in the multilayer films greatly influenced the loading conditions. MB molecules containing quaternary ammonium groups preferred to be entrapped in the polymer matrix when the pH was high because of the existence of strong electrostatic attractive forces associated with the charged free carboxylic groups on the PAA chains and weak repulsive forces from the quaternary ammonium groups on the side of the PDMIHPC–laponite nanocomposite. The weak polyelectrolyte PAA swelled because of the electrostatic repulsive forces between the PAA chains.[40] The carboxylic acid groups (—COOH) in the PAA chains would be converted

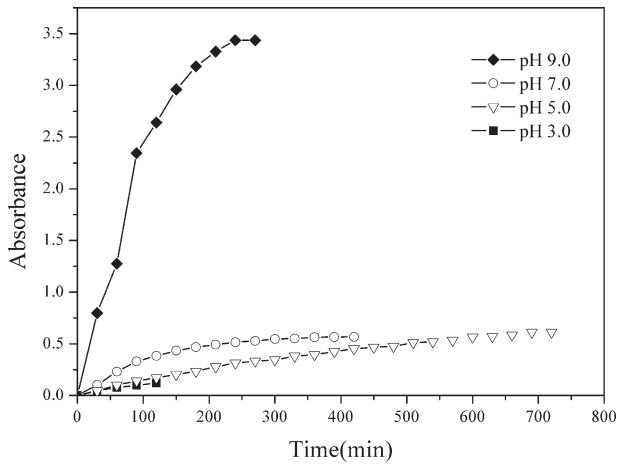

Figure 4. Effect of pH on the loading of MB from (PDMIHPC–laponite/PAA)$_{10}$ hydrogel nanocomposite films.

to negatively charged carboxylate groups (—COO$^-$) with increasing pH,[39] and the electrostatic repulsions between the —COO$^-$ groups led to the expansion of the chains and the swelling of the film. In addition, the hydrogel nanocomposite film had sufficient free space, so it could facilitate the incorporation of the guest materials. The core–shell structure of the film led to an increased amount of guest materials being loaded.

As shown in Figure 4, the loading amount and rate of MB increased when the pH value changed from 5.0 to 9.0. This was reasonable because the —COOH groups of the PAA were converted gradually to negatively charged —COO$^-$ groups,[41] and this promoted electrostatic attractive forces between the positively charged MB and —COO$^-$. Furthermore, the swelling of the film provided more free volume for the MB molecules to enter. This led to a faster loading rate. With the decrease in pH to 3.0, the loading capacity of the film became low. The —COOH groups of PAA at low pH reduced the repulsion and shrank the network. On the other hand, MB was protonized to be positively charged, and this caused stronger electrostatic repulsive forces between PDMIHPC–laponite and MB, which led to the lower loading amount of MB. The phenomenon was similar to that in Ding et al.'s[34] work, where the loading amount and rate of MB increased when the pH value was changed from 3.0 to 7.0. However, in contrast, the loading amount dropped down in his case when the pH was increased to 9.0 because the film started to dissolve because of the electrostatic screening effect of salt in alkali solution and electrostatic repulsive forces between the —COO$^-$ groups of the PAA chains. In our case, however, the film still remained intact because the core–shell structure of PDMIHPC–laponite could have been more tolerant to the salt effect after the laponite was introduced. The concentration of MB in the film was higher when the solution was more basic, whereas the minimum loading of MB occurred at low pH. This suggested that MB was loaded mainly through electrostatic forces of attraction in the film.

In our study, the MB loading capacity in the film was as large as about 4.48 μg/cm^2 per bilayer (the release data indicated ~672 μg of MB in 10 bilayers covering an area of 1500 mm^2). It was much larger than that of the polyurethane/PAA multilayer films (ca. 0.75 μg/cm^2 per bilayer). This confirmed that the core–shell structure made a contribution in a big capacity. It is worth mentioning that the loading reached equilibrium after 12 h at pH 5.0. A possible reason was that the conversion between —COOH groups and —COO$^-$ groups was in dynamic equilibrium because the pK_a of PAA was 4.25, and it would take a long time to reach conversion equilibrium. This also implied that MB was able to diffuse throughout the bulk of the film.

The effect of the ionic strength on the loading of MB from the (PDMIHPC–laponite/PAA)$_{10}$ multilayer films was also studied. The ionic strength was adjusted by NaCl when the pH of the solution was fixed to 9.0. Figure 5 shows the time dependence of the loading amount of MB in the film when the NaCl concentration was changed from 0 to 300 m*M*. The results indicate that the stronger ionic strength was, the lower the loading capacity and loading rate of MB was. The loading capacity and rate loss were often attributed to the screening effect of the salt.[42] The electrostatic repulsion between the positively charged PDMIHPC–laponite or natively charged PAA was progressively screened by the increase in the ionic strength. In addition, the salt also weakened the electrostatic interactions between the MB molecules and —COO$^-$ groups.[43,44] The equilibrium time increased from 4.5 to 8.5 h when the concentration of the NaCl solution was increased from 0 to 150 m*M*. However, the time was shortened to 4.5 h in the 300 m*M* NaCl solution. This was simply because the film showed a much lower swelling.

We also prepared (PDMIHPC–laponite/PAA)$_{10.5}$ multilayer films to observe the effect of the outermost layer of the film on the amount of MB loaded. The films were put into solution of MB at pH 9.0 to reach a saturation loading. In contrast, the (PDMIHPC–laponite/PAA)$_{10.5}$ film loaded a greater amount of dyes (Figure 6). The outermost layer was composed of PDMIHPC–laponite, which introduced more cavities into the film. As a result, more MB molecules could enter the large space in the structure. It took less time to reach loading equilibrium in the absence of a permeation barrier through PAA.

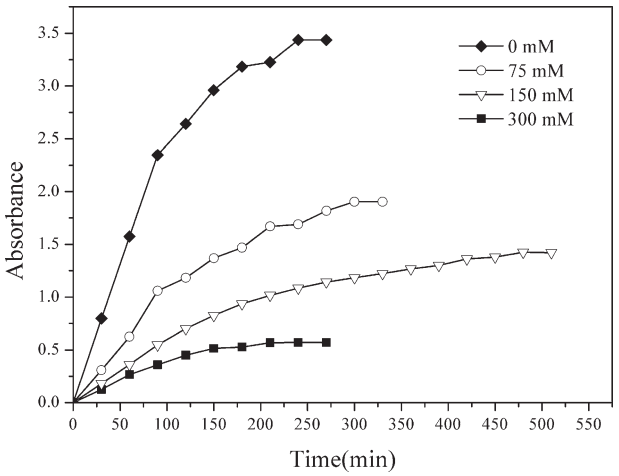

Figure 5. Effect of the ionic strength on the loading of MB from the (PDMIHPC–laponite/PAA)$_{10}$ hydrogel nanocomposite films.

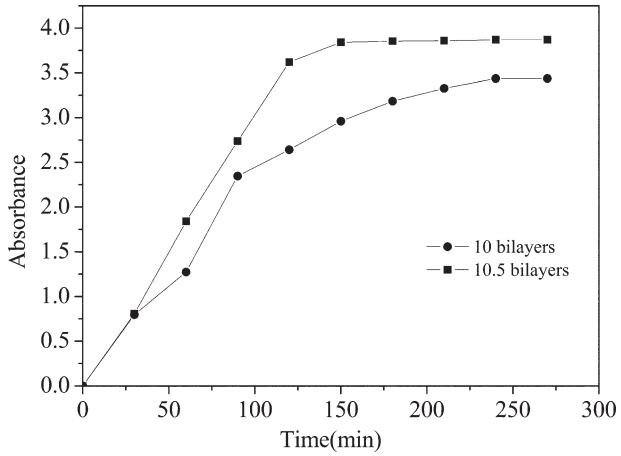

Figure 6. Effect of the number of layers on the loading of MB from the (PDMIHPC–laponite/PAA)$_n$ hydrogel nanocomposite films.

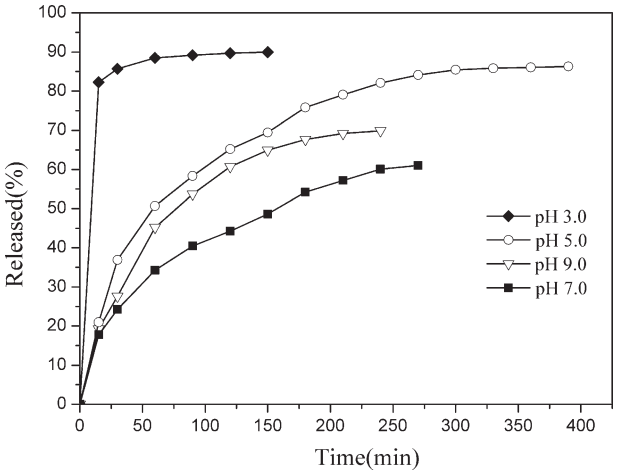

Figure 7. Effect of pH on the release of MB from the (PDMIHPC–laponite/PAA)$_{10}$ hydrogel nanocomposite films.

The process of MB diffusing into the film could be treated with the Fickian diffusion model. The equation for diffusion is expressed as follows:[45,46]

$$\ln\left(1-\frac{I_{ul}}{I_{ul\infty}}\right)=\ln\left(\frac{8}{\pi^2}\right)-\frac{D\pi^2}{d^2}t \qquad (1)$$

where I_{ul} and $I_{ul\infty}$ are the adsorbances from the absorbed MB molecules at time t and ∞, respectively (i.e., when the intensity approached a constant value), and were obtained with UV–vis measurements and d is the thickness of the film. D is the diffusion coefficient and the produced diffusion coefficients (D_s) are listed in Table I. The value of D_s confirmed the previous conclusion. The values of D_s increased when the pH was changed from 5.0 to 9.0. This indicated that the loading rate of MB increased. In the ionic strength case, the values of D_s decreased when the concentration of NaCl solution changed from 0 to 150 m*M*. This confirmed that the loading rate decreased with increasing ionic strength. However, the values of D_s at pH 3 or an NaCl concentration of 300 m*M* were observed to be against the previous rules. This could be explained by the fact that the swelling process played a dominant role in the loading process.

Release of MB

As show in Figure 7, it was clear that the release rates increased with decreasing pH when the concentration of NaCl in all of the solutions was 75 m*M*. This was also observed the few MB molecules released from the film in pure water. The process of release involved two major processes: an initial burst in the first hours and a steady release at later times. Nearly 90% of MB was released at pH 3.0, and it took about 2.5 h to reach the saturation point of release. Because the electrostatic interactions between MB and —COO— groups were broken at pH 3.0, a large amount of H^+ penetrated into the film and then interacted with —COO— groups on the PAA chains.[47] These factors were for the cause of the greater amount of MB released. In contrast, the release process lasted 7 h at pH 5.0. The —COOH groups were inclined to ionize gradually with increasing pH from 5.0 to 9.0, and the electrostatic repulsive forces between the —COO— groups of the PAA chains increased; this could facilitate to a large extent the swelling of the film.[40] However, it is worth mentioning that the release of MB at pH 9.0 did not decrease further. This fact suggested that the cavity within the film imprisoned the MB in addition to the electrostatic forces. It is well known that the pH varies along the gastrointestinal tract. Thus, pH is the one of the important factors in the releasing process. It may be possible to design pH-triggered drug-delivery systems. A drug could be embedded in LbL films and released upon changes in the pH.

It could be clearly seen that the release amount and rate of MB was higher and faster with increasing ionic strength (Figure 8). The release process could last about 3 h in the 300 m*M* NaCl solution, whereas it took 7 h to achieve release equilibrium in the 75 m*M* NaCl solution. The released amount reached 91.4% in the 300 m*M* NaCl solution; this was similar than that at pH 3.0 (Figure 7). The swelling of the film was closely related to the release process. As a result, the release rate increased gradually.[43] Jiao et al.[22] fabricated poly(lactic acid) nanoparticles, which encapsulated pyrene as a model drug, and poly(ethylene imine) (PEI) LbL films as a novel drug-delivery system. There was an initial burst in the first 20 h. They suggested that the films of poly(lactic acid) nanoparticles were promising for the sustained release of drugs. In our case, the swelling of the film

Table I. Calculated D_s Values for the Loading Process

	pH				Concentration of NaCl (mM)			
	3.0	5.0	7.0	9.0	0	75	150	300
D_s	0.017	0.0029	0.0102	0.0147	0.0138	0.0092	0.0063	0.0124
R^2	0.9994	0.9937	0.9986	0.9791	0.9901	0.9855	0.9996	0.9998

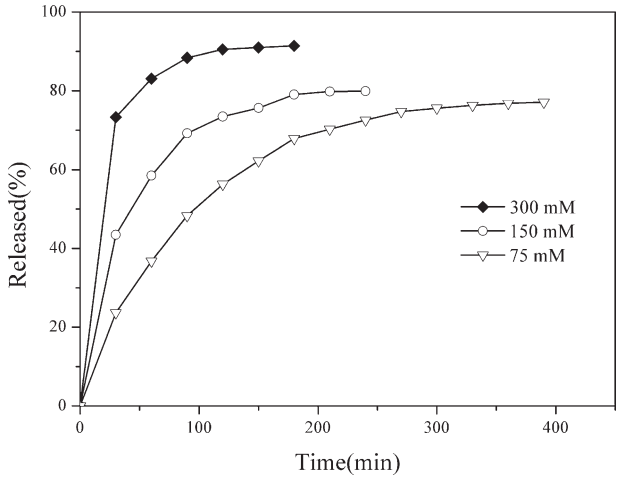

Figure 8. Effect of the ionic strength on the release of MB from the $(PDMIHPC–laponite/PAA)_{10}$ hydrogel nanocomposite films.

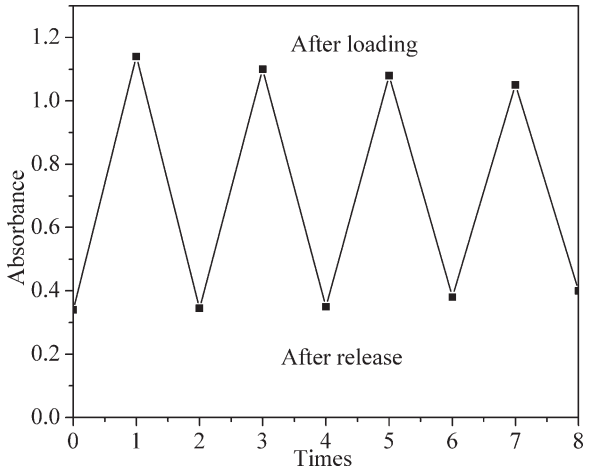

Figure 9. Reversibility of the loading-release of MB from the $(PDMIHPC–laponite/PAA)_{10}$ hydrogel nanocomposite films.

in solution played an important role in the release process. This indicated that MB release was also ionic-strength-controlled process.

The release kinetics of MB from the film were analyzed with the follow equation:[48,49]

$$\ln\left(\frac{M_t}{M_\infty}\right) = \ln k + n \ln t \quad (2)$$

where M_t and M_∞ are the amounts of MB released from the film at time t and ∞, k is a constant related to the structure of the films, and n is a characteristic index that determines the type of release. If n is lower than 0.5, it is a Fickian diffusion mechanism. Otherwise, it is a non-Fickian diffusion mechanism. As shown in Table II, each value of n was lower than 0.5, so all of them were Fickian diffusion mechanisms. An increase in k from pH 9 to 3 indicated that the diffusion rate was faster in the acidic solution. In contrast, a faster rate was found at higher concentrations of NaCl because of the larger k.

A greater observation from this study was that it was possible to essentially trap about 10% of the dye molecules in the films under pH 3 or an NaCl concentration of 300 m*M*. To test the validity of this trapping phenomenon, films were immersed in the solutions at the appropriate pH values and concentrations of NaCl for a period of 3 weeks with rather little change in the amount of MB retained in the films. The high concentration of MB molecules in the films and the strong electrostatic attractions existing between the MB molecules and the functional groups in the film under certain pH and ionic strength conditions promoted a high degree of aggregation of the molecules. It was thought that the combination of strong attractive interactions reduced repulsive forces, and the large extent of dye aggregation contributed to the retention of the dye molecules.

Reversible Loading and Release of MB

The reversible loading and release properties of the $(PDMIHPC–laponite/PAA)_{10}$ hydrogel nanocomposite films was investigated. The film was immersed in a 0.1 mg/mL MB solution at pH 9.0 for 5 h. Then, we rinsed it to remove excess dyes and dried it. In the second step, the MB-loaded film was put into 300 m*M* NaCl at pH 3.0 for 3 h. We repeated the process alternately for the desired times (Figure 9). We observed that the absorbance changed regularly. After eight cycles of loading and release, the film changed but only a little. This showed that the film was stable and could be used as a material in drug delivery.

Svetlane et al.[50] studied the release mechanisms in terms of three different processes: a diffusion-controlled process, film degradation, and triggered controlled release. Our experimental results fit the triggered released mechanism. The film was stable in a wide range of pH values, and the pH value of the immersed solution influenced the loading and release behavior, so a fine pH-triggered reversible loading and release system was successfully constructed.

Scanning electron microscopy (SEM) was used to gain further insight into the changes in the film structure. Figure 10(a) shows a wrinkle surface of the 10-bilayer film. The film thickness was estimated by the SEM imaging of the cross-sectional view of the film. As shown in Figure 10(b), the (PDMIHPC–

Table II. Release Kinetics Data of MB from the Film for the Release Process

	pH				Concentration of NaCl (mM)		
	3.0	5.0	7.0	9.0	75	150	300
n	0.0417	0.4296	0.4327	0.4803	0.4877	0.3341	0.1559
k	0.8218	0.0911	0.092	0.0808	0.0651	0.1817	0.4754
R^2	0.9631	0.9611	0.997	0.9685	0.962	0.9672	0.9854

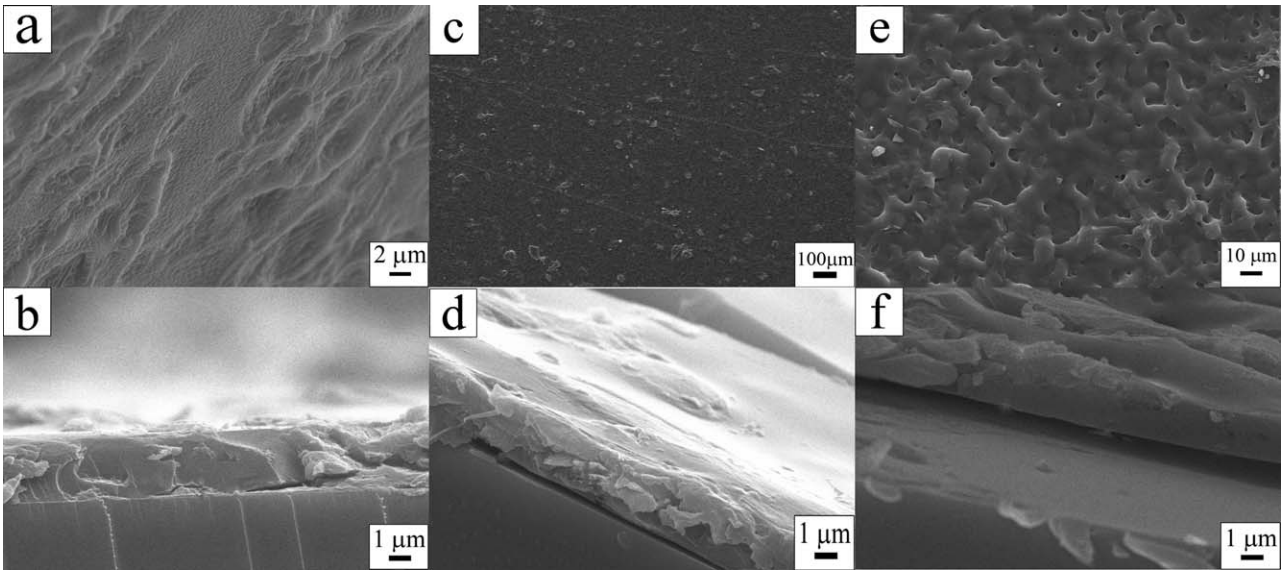

Figure 10. SEM images of the (PDMIHPC–laponite/PAA)$_{10}$ hydrogel nanocomposite films: (a) surface of the film, (b) surface of film after the loading of MB, (c) surface of the film after the release of MB, (d) cross section of the film before the loading of MB, (e) cross section of the film after the loading of MB, and (f) cross section of the film after the release of MB.

laponite/PAA)$_{10}$ film before MB loading had a constant thickness of 2.89 μm. After the saturation loading of MB, there was some uneven distribution of the region on the film's surface [Figure 10(c)]. It was assumed that this was caused by the aggregation of MB molecules. The upper part of Figure 10(d) shows a greatly enlarged view of the film after the loading of MB. Interestingly, we found that the film thickness turned out to be thinner after loading. The thickness was only 1.88 μm [Figure 10(d)]. This phenomenon further proved the uniform structure of the hydrogel nanocomposite film. MB combined with the —COO— groups of the PAA chains reduced the electrostatic repulsive forces. In comparison, the surface became rough and porous after the release of MB [Figure 10(e)]. The feature caused by the penetration of MB molecules from the film, and the components of the LbL film were swollen in acidic solution. So, after MB was released from the film, the thickness of the film increased back to 2.58 μm [Figure 10(f)], and the film structure was almost recovered. All of the images provided strong evidence that MB could migrate across the outside layers and then interact with PAA by electrostatic attraction. The interaction and spaces played a leading role in the loading and release processes.

Recently, we obtained LbL free-standing films from the substrates. The tensile strength of the free-standing films was about 2 MPa. More work on the mechanical properties is in progress.

CONCLUSIONS

In this study, a PDMIHPC–laponite nanocomposite with a core–shell structure was used as one of components of an LbL film. A thin hydrogel nanocomposite film was constructed by the alternative deposition of PDMIHPC–laponite and PAA. The procedure fitted linear growth that could be described as $d = 109.3n - 359.7$ $(n = 4–10)$. The hydrogel nanocomposite film showed an extraordinary loading MB capacity as large as about 4.48 $\mu g/cm^2$ per bilayer at pH 9.0. Nearly 90% of MB was released at pH 3.0 or in a 300 m*M* NaCl solution. The outmost layer of assembled layers showed a significant effect on the loading ability of the film. The loading and release abilities of MB from the (PDMIHPC–laponite/PAA)$_{10}$ film could be tuned by pH and the salt concentration of the medium. The loading rate was faster at the high pH values or low salt concentration, whereas the release rate exhibited a contrary trend. This hydrogel nanocomposite film could be an advanced material for applications in triggered controlled release systems.

ACKNOWLEDGMENTS

This work was supported by the National Natural Science Foundation of China (contract grant number 51163015) and the Program for New Century Excellent Talents in University (contract grant number NCET-11–1072).

In this study, Shimei Xu conceived the experiments, Renbao Gu synthesized the film and wrote the article, Huili Li performed the measurement experiments, Xinglin Yuan prepared the figures, Jide Wang and Ronglan Wu did the data analysis, and all of the authors discussed the results and commented on the article at all stages.

REFERENCES

1. Langer, R. *Science* **1990**, *249*, 1527.
2. Chung, A. J.; Rubner, M. F. *Langmuir* **2002**, *18*, 1176.
3. Ariga, K.; Hill, J. P.; Ji, Q. *Phys. Chem. Chem. Phys.* **2007**, *9*, 2319.
4. Decher, G. *Science* **1997**, *277*, 1232.
5. Gribova, V.; Auzely-Velty, R.; Picart, C. *Chem. Mater.* **2011**, *24*, 854.

6. Podsiadlo, P.; Michel, M.; Lee, J.; Verploegen, E.; Wong Shi Kam, N.; Ball, V.; Lee, J.; Qi, Y.; Hart, A. J.; Hammond, P. T.; Kotov, N. A. *Nano Lett.* **2008**, *8*, 1762.
7. Wang, L.; Wang, Z.; Zhang, X.; Shen, J.; Chi, L.; Fuchs, H. *Macromol. Rapid Commun.* **1997**, *18*, 509.
8. Kharlampieva, E.; Erel-Unal, I.; Sukhishvili, S. A. *Langmuir* **2006**, *23*, 175.
9. Lutkenhaus, J. L.; Hrabak, K. D.; McEnnis, K.; Hammond, P. T. *J. Am. Chem. Soc.* **2005**, *127*, 17228.
10. Inoue, H.; Sato, K.; Anzai, J.-I. *Biomacromolecules* **2004**, *6*, 27.
11. Serizawa, T.; Kamimura, S.; Kawanishi, N.; Akashi, M. *Langmuir* **2002**, *18*, 8381.
12. Ajiro, H.; Beckerle, K.; Okuda, J.; Akashi, M. *Langmuir* **2012**, *28*, 5372.
13. Wang, X.; Zhang, L.; Wang, L.; Sun, J.; Shen, J. *Langmuir* **2010**, *26*, 8187.
14. Zhang, X.; Shi, F.; Yu, X.; Liu, H.; Fu, Y.; Wang, Z.; Jiang, L.; Li, X. *J. Am. Chem. Soc.* **2004**, *126*, 3064.
15. Almodóvar, J.; Place, L. W.; Gogolski, J.; Erickson, K.; Kipper, M. *J. Biomacromolecules* **2011**, *12*, 2755.
16. Zhang, X.; Shi, F.; Niu, J.; Jiang, Y.; Wang, Z. *J. Mater. Chem.* **2008**, *18*, 621.
17. Lvov, Y.; Ariga, K.; Ichinose, I.; Kunitake, T. *J. Am. Chem. Soc.* **1995**, *117*, 6117.
18. Ren, K.; Wang, Y.; Ji, J.; Lin, Q.; Shen, J. *Colloids Surf. B* **2005**, *46*, 63.
19. Zhao, N.; Shi, F.; Wang, Z.; Zhang, X. *Langmuir* **2005**, *21*, 4713.
20. Zhang, L.; Liu, H.; Zhao, E.; Qiu, L.; Sun, J.; Shen, J. *Langmuir* **2012**, *28*, 1816.
21. Bassim, N. D.; Dressick, W. J.; Fears, K. P.; Stroud, R. M.; Clark, T. D.; Petrovykh, D. Y. *J. Phys. Chem. C* **2012**, *116*, 1694.
22. Jiao, Y. H.; Li, Y.; Wang, S.; Zhang, K.; Jia, Y. G.; Fu, Y. *Langmuir* **2010**, *26*, 8270.
23. Lee, S. W.; Kim, B. S.; Chen, S.; Shao-Horn, Y.; Hammond, P. T. *J. Am. Chem. Soc.* **2009**, *131*, 671.
24. Podsiadlo, P.; Kaushik, A. K.; Arruda, E. M.; Waas, A. M.; Shim, B. S.; Xu, J.; Nandivada, H.; Pumplin, B. G.; Lahann, J.; Ramamoorthy, A. *Science* **2007**, *318*, 80.
25. Mamedov, A. A.; Kotov, N. A. *Langmuir* **2000**, *16*, 5530.
26. Delcea, M.; Möhwald, H.; Skirtach, A. G. *Adv. Drug Delivery Rev.* **2011**, *63*, 730.
27. Liu, Z.; Yi, Y.; Gauczinski, J.; Xu, H.; Schönhoff, M.; Zhang, X. *Langmuir* **2011**, *27*, 11806.
28. Caruso, F.; Caruso, R. A.; Möhwald, H. *Science* **1998**, *282*, 1111.
29. Abalde-Cela, S.; Ho, S.; Rodríguez-González, B.; Correa-Duarte, M.; Álvarez-Puebla, R.; Liz-Marzán, L.; Kotov, N. *Angew. Chem. Int. Ed.* **2009**, *48*, 5326.
30. Kozlovskaya, V.; Kharlampieva, E.; Khanal, B. P.; Manna, P.; Zubarev, E. R.; Tsukruk, V. V. *Chem. Mater.* **2008**, *20*, 7474.
31. Poon, Y. F.; Cao, Y.; Liu, Y.; Chan, V.; Chan-Park, M. B. *Am. Chem. Soc. Appl. Mater. Int.* **2010**, *2*, 2012.
32. Yamanlar, S.; Sant, S.; Boudou, T.; Picart, C.; Khademhosseini, A. *Biomaterials* **2011**, *32*, 5590.
33. Wang, L.; Wang, X.; Xu, M.; Chen, D.; Sun, J. *Langmuir* **2008**, *24*, 1902.
34. Ding, C.; Xu, S.; Wang, J.; Liu, Y.; Hu, X.; Chen, P.; Feng, S. *Polym. Adv. Technol.* **2011**, *23*, 1283.
35. Fei, X.; Lin, J.; Wang, J.; Lin, J.; Shi, X.; Xu, S. *Polym. Adv. Technol.* **2012**, *23*, 736.
36. Liu, D.; Liu, H.; Hu, N. *Electrochim. Acta* **2010**, *55*, 6426.
37. Elbert, D. L.; Herbert, C. B.; Hubbell, J. A. *Langmuir* **1999**, *15*, 5355.
38. Choi, I.; Suntivich, R.; Plamper, F. A.; Synatschke, C. V.; Mueller, A. H. E.; Tsukruk, V. V. *J. Am. Chem. Soc.* **2011**, *133*, 9592.
39. Caruso, F.; Lichtenfeld, H.; Donath, E.; Möhwald, H. *Macromolecules* **1999**, *32*, 2317.
40. Ruths, J.; Essler, F.; Decher, G.; Riegler, H. *Langmuir* **2000**, *16*, 8871.
41. Ibarz, G.; Dähne, L.; Donath, E.; Möhwald, H. *Adv. Mater.* **2001**, *13*, 1324.
42. Steitz, R.; Leiner, V.; Siebrecht, R.; Klitzing, R. V. *Colloids Surf. A.* **2000**, *163*, 63.
43. Sukhorukov, G. B.; Schmitt, J.; Decher, G. *Ber. Bunsen-Ges. Phys. Chem.* **1996**, *100*, 948.
44. Klitzing, R. V.; Möhwald, H. *Macromolecules* **1996**, *29*, 6901.
45. Kara, S.; Gacal, B.; Tunc, D.; Yagci, Y.; Pekcan, Ö. *J. Fluores.* **2012**, *22*, 1073.
46. Ataman, E.; Pekcan, Ö. *J. Macromol. Sci. Phys.* **2007**, *46*, 705.
47. Tedeschi, C.; Caruso, F.; Möhwald, H.; Kirstein, S. *J. Am. Chem. Soc.* **2000**, *122*, 5841.
48. Evingür, G. A.; Pekcan, Ö. *Adv. Compos. Mater.* **2012**, *21*, 193.
49. Berg, M. C.; Zhai, L.; Cohen, R. E.; Rubner, M. F. *Biomacromolecules* **2006**, *7*, 357.
50. Pavlukhina, S.; Sukhishvili, S. *Adv. Drug Delivery Rev.* **2011**, *63*, 822.